Molecular Architecture and Connectivity of the Budding Yeast Mtw1 Kinetochore Complex

Peter Hornung[1], Michael Maier[1], Gregory M. Alushin[2], Gabriel C. Lander[3], Eva Nogales[3,4,5] and Stefan Westermann[1]*

[1]*Research Institute of Molecular Pathology, Dr. Bohr Gasse 7, 1030 Vienna, Austria*
[2]*Biophysics Graduate Group, University of California, Berkeley, Berkeley, CA 94720, USA*
[3]*Life Science Division, Lawrence Berkeley National Laboratory, 1 Cyclotron Road, Berkeley, CA 94720, USA*
[4]*Department of Molecular and Cell Biology, University of California, Berkeley, Berkeley, CA 94720, USA*
[5]*Howard Hughes Medical Institute, Chevy Chase, MD, USA*

Kinetochores are large multiprotein complexes that connect centromeres to spindle microtubules in all eukaryotes. Among the biochemically distinct kinetochore complexes, the conserved four-protein Mtw1 complex is a central part of the kinetochore in all organisms. Here we present the biochemical reconstitution and characterization of the budding yeast Mtw1 complex. Direct visualization by electron microscopy revealed an elongated bilobed structure with a 25-nm-long axis. The complex can be assembled from two stable heterodimers consisting of Mtw1p–Nnf1p and Dsn1p–Nsl1p, and it interacts directly with the microtubule-binding Ndc80 kinetochore complex via the centromere-proximal Spc24/Spc25 head domain. In addition, we have reconstituted a partial Ctf19 complex and show that it directly associates with the Mtw1 complex *in vitro*. Ndc80 and Ctf19 complexes do not compete for binding to the Mtw1 complex, suggesting that Mtw1 can bridge the microtubule-binding components of the kinetochore to the inner centromere.

Introduction

Interaction between chromosomes and spindle microtubules requires the action of a complex multiprotein machine termed the kinetochore.[1,2] Kinetochores are responsible for microtubule-based force generation that drives sister chromatid separation in anaphase. They additionally contain an error-correction mechanism that ensures the bipolar attachment of sister chromatids to opposite spindle poles,[3] and they relay signals to the mitotic checkpoint that prevents the cell from entering anaphase in the presence of unattached kinetochores.[4] In budding yeast, the structural core of the kinetochore consists of at least seven biochemically distinct subcomplexes that are present in fixed copy numbers in mature budding yeast kinetochores[5] and assemble on centromeric DNA in a hierarchical manner.[6] A current challenge in the field is to elucidate the architecture of the kinetochore by defining the binding interfaces between kinetochore complexes. Previous biochemical studies have focused on the reconstitution and functional analysis of two important parts of the budding yeast outer kinetochore: the Dam1 complex and the Ndc80 complex. Both of these complexes directly interact with microtubules and are required for force generation in yeast kinetochores.[7,8] The Dam1 complex has the ability to oligomerize into rings *in vitro*,[9,10] opening up the possibility that a Dam1 ring is a physiologically relevant coupling

device for kinetochores on microtubule plus ends in yeast. Recent experiments have demonstrated that Dam1 is a specialized plus-end tracking complex required for a persistent attachment of the Ndc80 complex to dynamic microtubule ends *in vitro*.[11,12]

The four-protein 180-kDa Ndc80 complex is a conserved component of all kinetochores. Biochemical isolations from extracts and *in vitro* reconstitution experiments using *Caenorhabditis elegans* Ndc80 subunits have demonstrated that the complex functions together with the conserved four-protein complex Mtw1 (also called Mis12 or MIND) and with the protein KNL-1/Blinkin (Spc105p in budding yeast) as part of a larger network termed KMN (*K*NL-1 *M*is12 *N*dc80).[13] Analysis of temperature-sensitive mutants of MTW1 complex subunits in fission yeast and budding yeast, as well as depletion experiments in worms and human cells, has demonstrated that the complex is essential for kinetochore biorientation and chromosome segregation.[14–16] Since biochemical reconstitution experiments have so far only been performed with *C. elegans* kinetochore proteins, it is an open question whether the architecture, topology, and biochemical activities of the KMN network are conserved among evolutionarily distinct eukaryotes. Furthermore, it is unknown how the KMN network is anchored to the inner kinetochore, a critical step in creating a microtubule attachment site specifically at the centromere. Here, we report the reconstitution and biochemical characterization of the budding yeast Mtw1 complex. Our analysis defines the architecture of this central kinetochore complex and is an important step towards a reconstitution of the full yeast kinetochore.

Results and Discussion

Reconstitution of the four-protein Mtw1 complex

To reconstitute the budding yeast Mtw1 complex, we employed a polycistronic expression strategy. Genes encoding all four subunits (DSN1, MTW1, NNF1, and NSL1) of the complex were placed under the control of a T7 promoter and expressed in BL21 (DE3) cells. The purification strategy used a 6×His tag on the Nnf1p subunit, allowing initial purification with a Ni-NTA resin. After elution, the complex was further purified by size-exclusion chromatogra-

phy (SEC) (Fig. 1a). Analysis of the complex on Coomassie-stained gels revealed that all four subunits of the complex were present at a stoichiometry of 1:1:1:1. The complex eluted earlier than expected from SEC with a Stokes radius of 74.3 Å. The sedimentation coefficient of the Mtw1 complex was determined by glycerol gradient centrifugation and estimated to be 6S (data not shown). Thus, the native molecular mass of the recombinant complex is 183 kDa, compared to the calculated molecular mass of 148 kDa, and the frictional coefficient f/f_0 is 2.0, predicting a complex that is moderately to highly elongated. These values are in close agreement to those obtained for the Mtw1 complex in yeast extracts,[17] suggesting that the recombinant complex closely resembles its native counterpart. We noticed that the Dsn1p subunit of the complex was particularly prone to proteolytic degradation during purification (Fig. 1a). Sequencing of the major proteolysis products revealed that the N-terminus of Dsn1p is easily cleaved. We subsequently cloned an N-terminally shortened version of the Dsn1 subunit corresponding to the major proteolysis product, which lacks amino acids 1–171. Expression of Dsn1$^{172–567}$, in combination with full-length MTW1, NNF1-6×His, and NSL1, allowed the purification of the entire four-protein Mtw1 complex (Fig. 1b). We conclude that the N-terminal extension of Dsn1, which is unusually long in budding yeast compared to other eukaryotes and is predicted to be unstructured, is dispensable for complex formation *in vitro*. To determine whether this N-terminal extension has an essential function *in vivo*, we expressed wild-type or N-terminally truncated DSN1$^{172–576}$ on centromeric plasmids in a haploid DSN1 deletion strain that was kept viable by containing a wild-type copy of DSN1 on a CEN-based URA plasmid. Selection against the URA plasmid on 5-fluoroorotic acid plates demonstrated that Dsn1$^{172–576}$ supported wild-type growth (Supplementary Fig. 1). Thus, the N-terminal 172 amino acids of Dsn1 are not required for complex formation *in vitro* and do not have an essential function *in vivo*.

The Mtw1 complex can be assembled from two stable heterodimers

SEC analysis of epitope-tagged kinetochore proteins in yeast extracts suggests that Dam1 and Ndc80 complexes are present only in their fully assembled

Fig. 1. Reconstitution of the Mtw1 complex. (a) Expression and purification of the Mtw1 complex. The Coomassie-stained gel shows different steps of the purification scheme: control extract and extract after induction with IPTG, eluate from Ni-NTA beads, and purified fraction after SEC. Note the presence of the degradation products of the Dsn1p subunit. (b) Expression and purification of a complex with an N-terminally truncated Dsn1p subunit. (c) Expression and purification of a stable Dsn1–Nsl1 heterodimer. IEX denotes anion-exchange chromatography. Asterisks in (a), (b), and (c) indicate contamination with the *E. coli* Hsp70 chaperone. (d) Expression and purification of the Mtw1–Nnf1 heterodimer. (e) SEC runs of Dsn1p–Nsl1p and Mtw1p–Nnf1p subcomplexes (8 μM each) and of the full complex after reconstitution. (f) Coomassie-stained SDS-PAGE of fractions from (e). Asterisks indicate an Nnf1 truncation product.
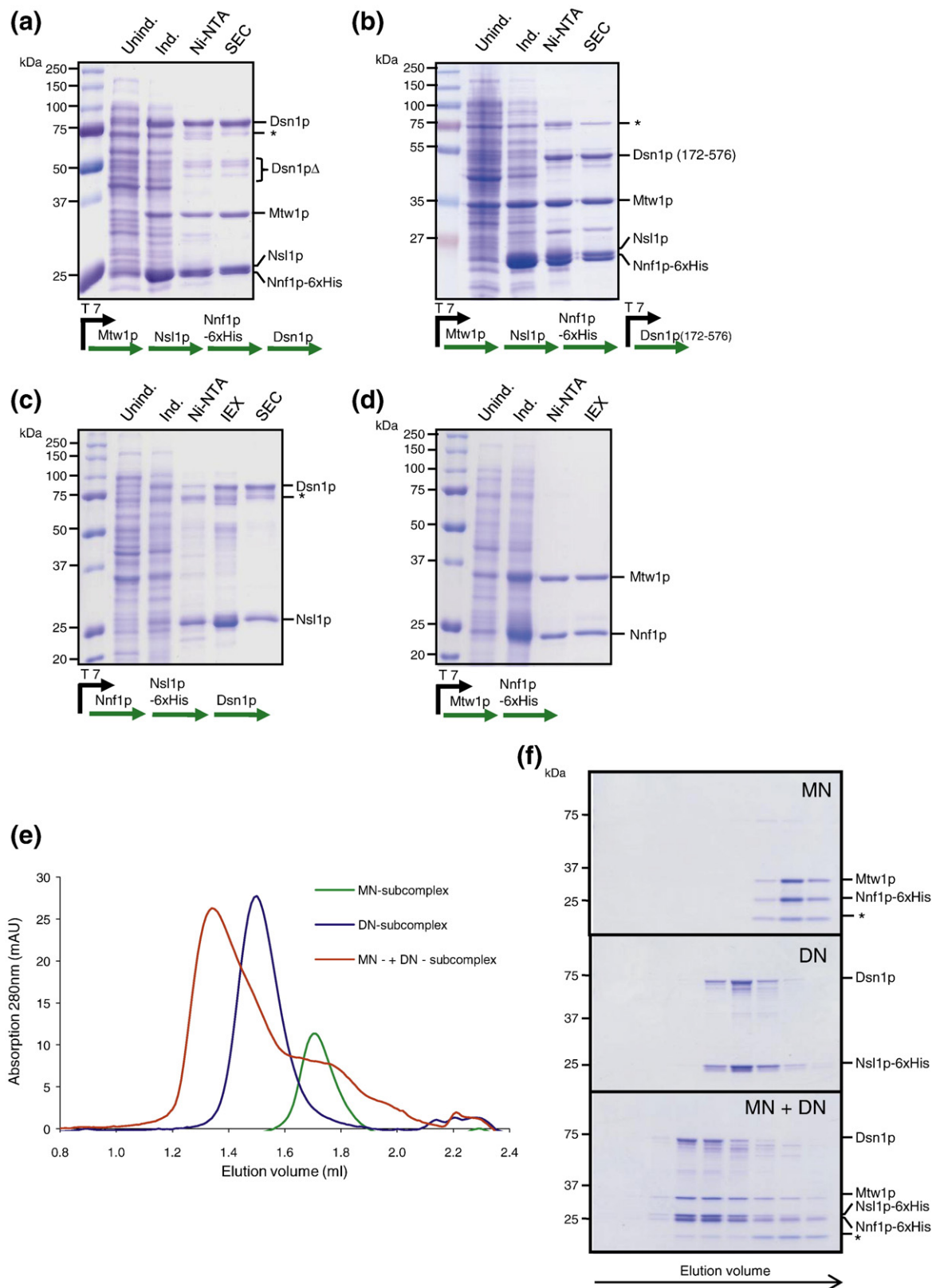
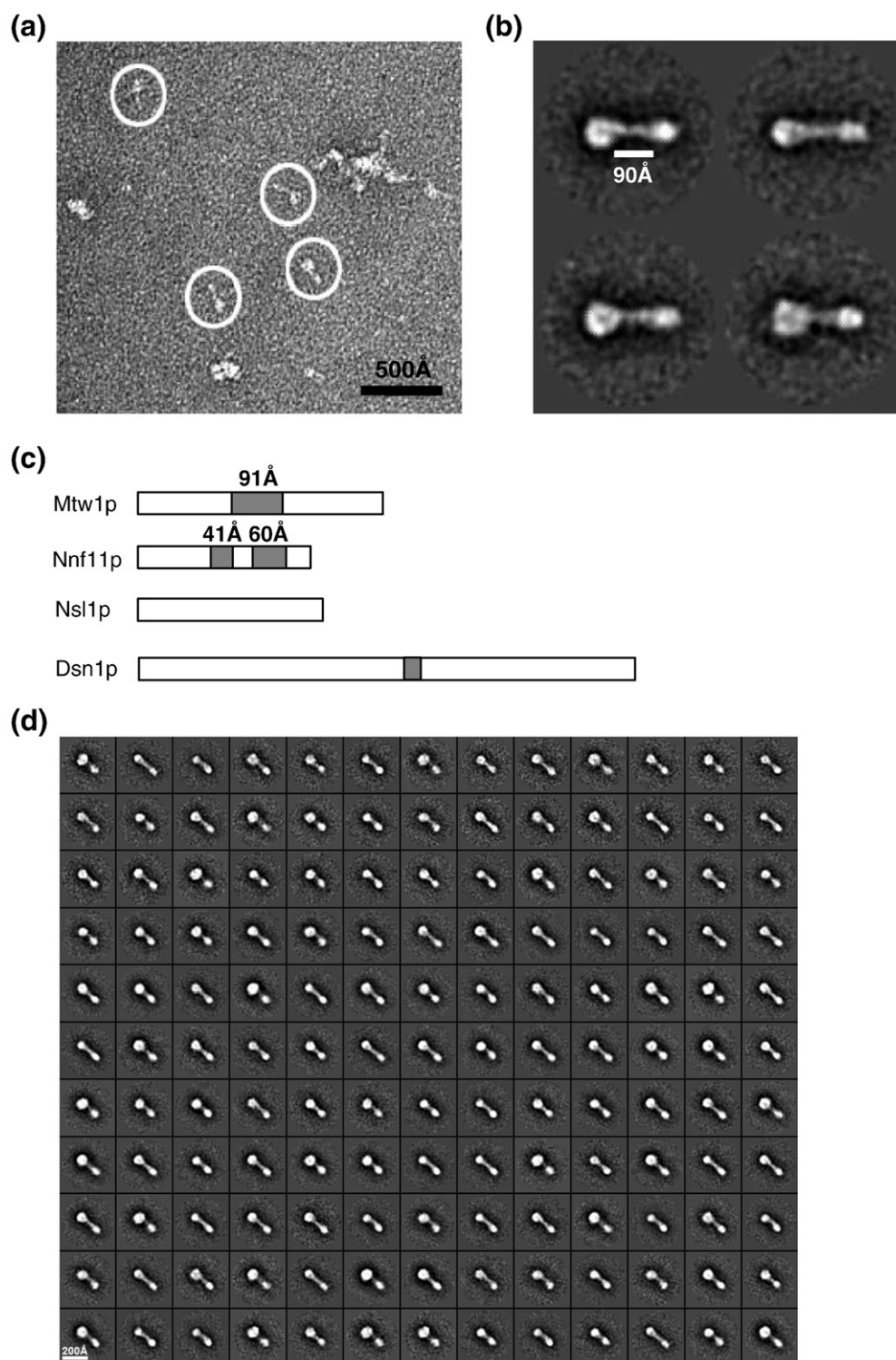**Fig. 1** (*legend on previous page*)

Fig. 2. EM analysis of the Mtw1 complex. (a) Negative-stain EM image of the Mtw1 complex. Note the heterogeneous composition of the sample. White circles correspond to particles chosen for further analysis. (b) Selected class averages showing the architecture and dimensions of the complex. The complex is a bilobed rod, with one large globular domain and one small globular domain. (c) Coiled-coil predictions for the protein subunits of the complex. Gray regions correspond to greater than 50% coiled-coil probability. (d) Entire complement of class averages obtained for the complex. They all display the bilobed architecture, with much heterogeneity occurring in the size of the larger globular domain.

state, although Mtw1 complexes of different compositions can be detected.[17] To identify such stable subcomplexes, we expressed various combinations of Mtw1 complex subunits. We were able to express and purify two stable complexes: a heterodimer consisting of Mtw1p and Nnf1p (MN complex) (Fig. 1d), and a heterodimer consisting of Dsn1p and Nsl1p (DN complex) (Fig. 1c). We next asked whether the Mtw1 heterotetramer can be reconstituted by combining the two stable dimers. After the mixing of MN and DN subcomplexes, followed by SEC, we observed a reconstitution of the full Mtw1 complex, which eluted at a position identical with that of the native complex (Fig. 1e). Thus, the four-protein Mtw1 complex is composed of two stable heterodimers consisting of Mtw1p–Nnf1p and Dsn1p–Nsl1p, a result that is in agreement with binary two-hybrid interactions between these subunits.[18]

Electron microscopy analysis of the reconstituted Mtw1 complex

Negative-stain single-particle electron microscopy (EM) was used to characterize the structural architecture of the Mtw1 complex. Despite our efforts to cross-link and purify the complex, the imaged fields of particles contained a heterogeneous mixture of aggregates and small fragments, as well as the monomeric full-size complex (Fig. 2a). We manually picked the particle images that appeared to correspond to the monomeric full-length complex based on their consistent size (Fig. 2a, white circles). After reference-free classification, we observed a distinct bilobed rod-like structure that is approximately 250 Å in length, with one of the lobes consistently appearing slightly larger than the other (Fig. 2b and d). The larger lobe varied in size, likely reflecting the presence of degrons in the Dsn1p subunit and/or different views around the long axis of the complex.

The larger globular lobe has an approximate diameter of 71 Å, and the smaller lobe has an approximate diameter of 47 Å. Assuming a spherical shape for each, this would correspond to an approximate mass of 150 kDa and 45 kDa, respectively, the sum of which (195 kDa) very closely matches the experimentally determined mass. The calculated mass of the smaller lobe matches well with the combined predicted masses of Mtw1p and Nnf1p (57 kDa), assuming that their coiled-coil domains project outwards from the lobe. The calculated mass of the larger lobe exceeds the combined masses of Dsn1p and Nsl1p (91 kDa), suggesting that this lobe deviates from spherical geometry (the smaller lobe is too small to accommodate the mass of this subcomplex). The thin density connecting the two globular lobes is approximately 90 Å long (Fig. 2b), which matches the length of a predicted dimeric coiled coil between the Mtw1p subunits and the Nnf1p subunits (Fig. 2c). We also experimentally demonstrated that these two proteins form a stable subcomplex, supporting the proposal that the coiled-coil regions of these two proteins probably dimerize in the context of the full complex. While this is the most parsimonious explanation for a complex topology, we cannot exclude the possibility that each globular head is occupied by more than two subunits.

In vivo, the Mtw1 complex acts as a bridge between the microtubule-binding Ndc80 complex and the inner kinetochore.[6] The Ndc80 complex is 57 nm in length,[19] and the Mtw1 complex is 25 nm in length. Taken together, these dimensions suggest that the KMN network is long enough to span the full length of the outer kinetochore, consistent with high-resolution fluorescence microscopy studies.[20]

Reconstitution of the interaction between Ndc80 complexes and Mtw1 complexes

We next asked whether the recombinant Mtw1 complex can directly interact with the Ndc80 complex. To this end, we purified the four-protein Ndc80 complex by expressing the Nuf2–Ndc80 and Spc24–Spc25 heterodimers individually and then reconstituted the entire complex using SEC (Fig. 3a). When the Mtw1 and Ndc80 complexes were mixed and subjected to gel filtration, the elution profile of the assembly was shifted with respect to the individual complexes. Coomassie-stained gels revealed that the complexes coeluted, and the densitometry of the Coomassie-stained bands indicated a 1:1 stoichiometry of the Mtw1–Ndc80 binary complex (Fig. 3b and c). The elution position indicated that the Ndc80–Mtw1 assembly is a dimer containing one copy of each complex. The Ndc80–Mtw1 stoichiometry obtained from this biochemical experiment is in agreement with quantitative fluorescence microscopy data indicating the presence of nearly identical numbers of Ndc80 (eight copies) and Mtw1 (six to seven copies) complexes for each budding yeast kinetochore.[5] Another important implication is that budding yeast Ndc80 and Mtw1 complexes form a stable association that does not depend on the presence of the KNL-1 protein Spc105p. This is in contrast to the *in-vitro*-reconstituted *C. elegans* KMN network, where only a Mis12–KNL-1 association is competent to interact with the Ndc80 complex.[13] Thus, while the overall association of Ndc80 and Mtw1 complexes is critical for the function of all kinetochores, the molecular details of this association can vary significantly in different organisms. Despite extensive efforts, we were unable to express sufficient amounts of full-length or partial KNL-1/Spc105p fragments, leaving open the possibility that the affinity of the Mtw1 complex for the Ndc80 complex may be increased by the presence of Spc105p.
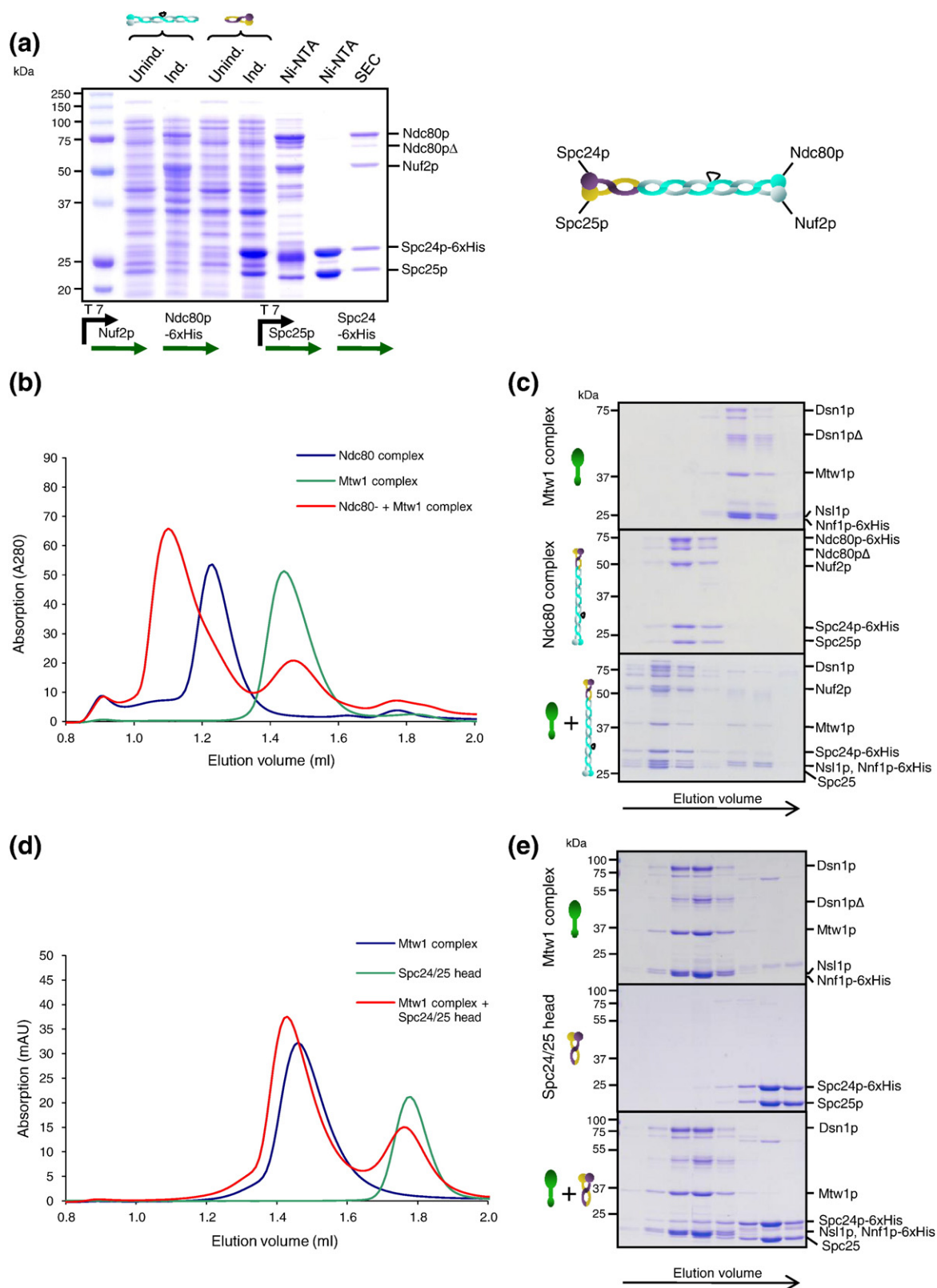
Fig. 3 (*legend on next page*)

The two globular domains of the Ndc80 complex have different functions: the Ndc80–Nuf2 head displays microtubule binding activity through the presence of two calponin homology domains and a basic N-terminal tail.[8,21] The Spc24/Spc25 head, on the other hand, is thought to reside proximal to the centromere and to connect the Ndc80 complex to the rest of the kinetochore. We tested which of the Ndc80 subcomplexes provides the binding site for the Mtw1 complex. Therefore, we subjected the purified Spc24/Spc25 head of the Ndc80 complex and the Mtw1 complex to SEC individually and then in combination. Upon preincubation with the Mtw1 complex, part of the isolated Spc24/Spc25 head was found coeluting with the Mtw1 complex (Fig. 3d and e). The interaction with the head domain seemed to be less efficient when compared to the full Ndc80 complex, suggesting that high affinity may require the full Ndc80 complex. We conclude that the Ndc80 complex directly binds to the Mtw1 complex via its centromere-proximal Spc24/Spc25 head domain, a result that is in agreement with high-resolution microscopy data placing Spc24/Spc25 in the immediate vicinity of Mtw1 complex subunits.[20]

Consistent with the results obtained for the *C. elegans* KMN network, the reconstituted Mtw1 complex did not bind directly to Taxol-stabilized microtubules in cosedimentation experiments (Supplementary Fig. 2). Only upon inclusion of the purified Ndc80 complex was the Ndc80–Mtw1 assembly found copelleting with microtubules. Furthermore, binding of the Mtw1 complex did not significantly alter the microtubule-binding properties of the Ndc80 complex (Supplementary Fig. 2).

A Ctf19 core complex directly associates with the Mtw1 complex

High-resolution colocalization data place the Mtw1 complex close to the centromere–kinetochore interface,[20] but the inner centromere receptor for the complex has not been identified. The human Mis12 complex has been reported to copurify and directly interact with the inner centromere protein HP1 via the human NSL1 subunit.[22,23] The importance of this interaction for mitotic kinetochore function, however, is unclear, and an HP1 homolog is absent from the *Saccharomyces cerevisiae* genome. Biochemical purifications of epitope-tagged Mtw1 subunits from yeast extracts[17,24] have suggested two candidate interaction partners at the inner centromere

interface: the budding yeast CENP-C homolog Mif2p and the Ctf19 complex. Initial experiments failed to detect a direct interaction between recombinant Mif2p fragments and the Mtw1 complex (data not shown), prompting us to focus on the Ctf19 complex as a potential binding partner. The yeast Ctf19 complex is the functional homolog of the constitutive centromere-associated network (CCAN) of higher eukaryotes. The CCAN was originally identified as a set of polypeptides that copurify with CENP-A-containing nucleosomes.[25,26] The budding yeast Ctf19 complex consists of at least 11 subunits, some of which are organized into more stable subcomplexes. We reconstituted a core Ctf19 complex consisting of the proteins Ctf19p, Okp1p, Mcm21p, and Ame1p (also termed COMA[17]) by coexpression in *Escherichia coli*. A purification procedure utilizing the 6×His-tagged Ame1p subunit allowed isolation of the four-protein complex to near homogeneity (Fig. 4a). Mcm21, Ame1-6×His, and Ctf19 polypeptides could be resolved on a 20-cm-long SDS-PAGE gel (Fig. 4a, right), and individual bands were excised and analyzed by mass spectrometry. This allowed assignment of the subunits to the corresponding bands on SDS-PAGE. The intensity of the Coomassie-stained bands suggests the presence of all four subunits of the COMA complex at a stoichiometry of 1:1:1:1.

To analyze potential associations with other kinetochore complexes, we immobilized different concentrations of FLAG-tagged COMA complex on beads; incubated them with recombinant Mtw1, Ndc80, and Dam1 kinetochore complexes; washed them; and subsequently eluted them with FLAG peptide (Fig. 4b). While we failed to detect a direct association of the purified COMA complex with recombinant Ndc80 and Dam1 complexes, the Mtw1 complex consistently coeluted with COMA in a concentration-dependent manner (Fig. 4c).

To verify a direct interaction between Mtw1 complexes and COMA complexes, we performed a reciprocal experiment in which 6×His-tagged Mtw1, Ndc80, and Dam1 complexes were each immobilized on Ni-NTA agarose, incubated with recombinant Ctf19–FLAG core complex, washed, and eluted with imidazole. Only in the presence of the Mtw1 complex is coelution of the COMA complex observed (Fig. 4c). To more stringently test the physical interaction, we analyzed the Mtw1 and COMA complexes by SEC and found that the complexes coeluted (Fig. 5). This result raises the possibility that

---

Fig. 3. The Mtw1 complex interacts with Ndc80 via the Spc24/Spc25 head. (a) Expression and purification of the Ndc80 kinetochore complex. The Ndc80–Nuf2 and Spc24–Spc25 heterodimers are expressed individually; in combination, the reconstituted full complex is purified by SEC. (b) Coomassie-stained gels of gel-filtration runs of the Mtw1 complex and the Ndc80 complex alone or in combination (9 μM each). (c) Gel-filtration profile corresponding to (b). (d) Coomassie-stained gels of the Mtw1 complex and the purified Spc24/Spc25 head domain alone or in combination (6 μM each). (e) Gel-filtration profile corresponding to (d).

COMA is involved in recruiting the Mtw1 complex to the inner centromere in budding yeast. A strong prediction from this hypothesis is that Ndc80 and COMA complexes should not compete for binding to the Mtw1 complex. We tested this by preincubating the Mtw1 and Ndc80 complexes, allowing formation of the binary Mtw1–Ndc80 assembly, followed by incubation with COMA–FLAG beads. Incubation
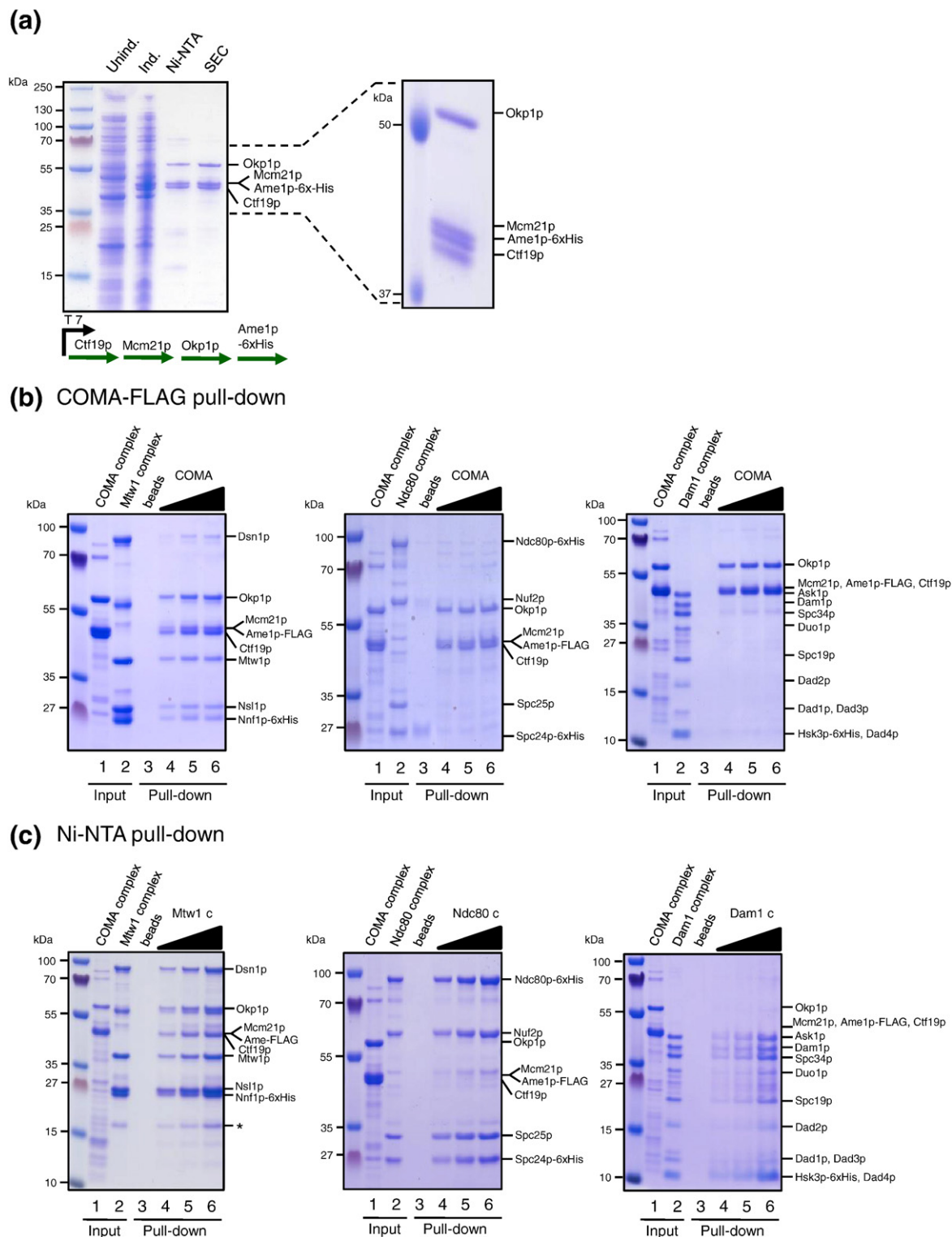

(a)

(b) COMA-FLAG pull-down

(c) Ni-NTA pull-down
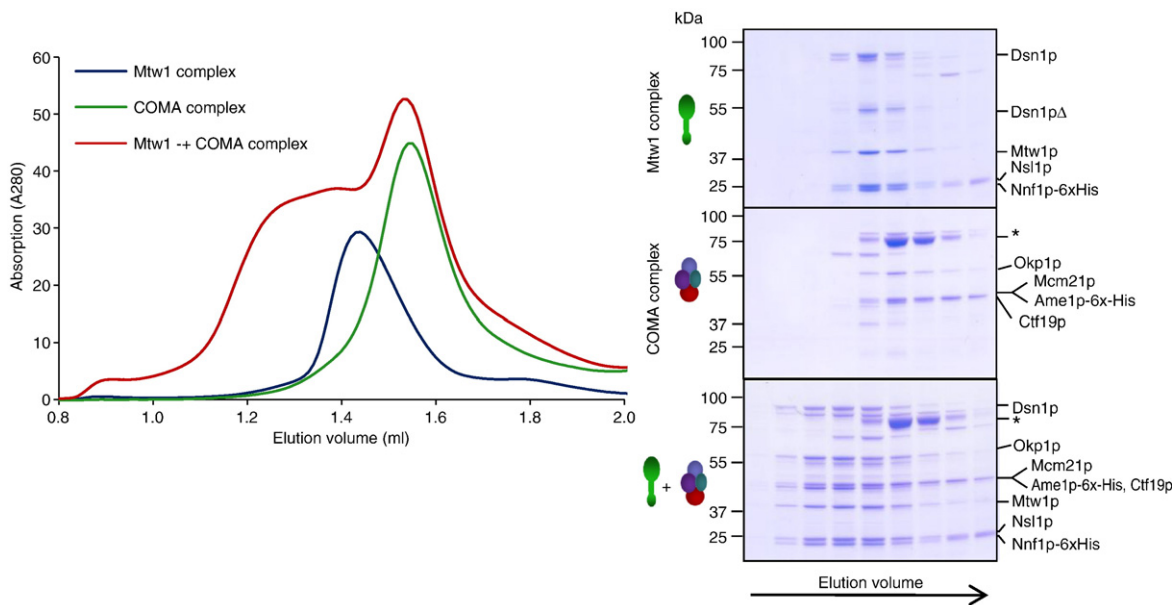
Fig. 4 (*legend on next page*)

Fig. 5. SEC of Mtw1 and COMA complexes. Coomassie-stained gels and gel-filtration profiles of the Mtw1 complex and the Ndc80 complex individually or in combination (5 μM each). Asterisk indicates Hsp70 contamination in the COMA complex sample.

with Ndc80 did not prevent the interaction between COMA complexes and Mtw1 complexes, and both complexes coeluted from the beads (Fig. 6a). This result indicates that the Ndc80 and COMA complexes occupy different binding sites on the Mtw1 complex. When testing the Mtw1–Nnf1 (MN) and Dsn1–Nsl1 (DN) subcomplexes separately in pull-down experiments, we found that the MN subcomplex interacted more efficiently with COMA (Fig. 6b and c). Interestingly, among all Mtw1 subunits, high-resolution colocalization data place Nnf1p closest to the inner centromere in both humans and *S. cerevisiae*.[27] Since the size of the smaller lobe of the Mtw1 complex roughly fits the combined masses of Mtw1–Nnf1, we tentatively speculate that the larger lobe, predominantly consisting of Dsn1p and Nsl1p, interacts with Spc24/Spc25, while the smaller lobe makes contact to the inner centromere COMA complex. Further antibody decoration experiments and direct visualization by EM will have to test this hypothesis.

In summary, we have characterized the basic architecture of the budding yeast Mtw1 complex. Very recently, two manuscripts have described the reconstitution of the yeast complex[28] and the human Mis12 complex.[29] Our independent results on the overall shape of the yeast Mtw1 complex as judged by EM, its assembly from two stable heterodimers, and the high-affinity interaction with the Ndc80 complex are in close agreement with the experiments performed by Maskell *et al.* A comparison to the human Mis12 complex reveals interesting similarities and differences: the overall architecture of the complex, with its topology based on stable Mtw1–Nnf1 and Dsn1–Nsl1 heterodimers, is conserved between yeast and human. However, the molecular mechanism by which a high-affinity interaction with the Ndc80 complex is achieved differs considerably between the two organisms. In particular, a yeast Dsn1–Nsl1 heterodimer alone is not competent to bind the Ndc80 complex (our unpublished observations). Yeast Nsl1 lacks a

Fig. 4. Reconstitution of a Ctf19 core complex (COMA) and interaction with Mtw1. (a) Reconstitution of the COMA complex. Coomassie-stained gel at different stages of purification. Right: The four polypeptides of the complex are resolved on large SDS-PAGE gels. (b) Pull-down experiment with immobilized COMA complex. Different amounts of recombinant COMA complex (lane 1) were immobilized on Anti-FLAG M2 Affinity Gel and incubated with the Mtw1, Ndc80, or Dam1 complex (lane 2). Control pull-downs contained only M2 beads (lane 3). After the bound complexes had been washed, they were eluted with FLAG peptide (lanes 4–6). Note that the Mtw1 complex coelutes with COMA from the beads. (c) The COMA–FLAG complex (lane 1) was incubated with His-tagged Mtw1, Ndc80, or Dam1 complexes, which were immobilized on Ni-NTA beads (lane 2; lane 3 denotes Ni-NTA beads as negative control). After the bound complexes had been washed, they were eluted with imidazole (lanes 4–6). Note that the COMA complex is coeluted with the Mtw1 complex from Ni-NTA beads.
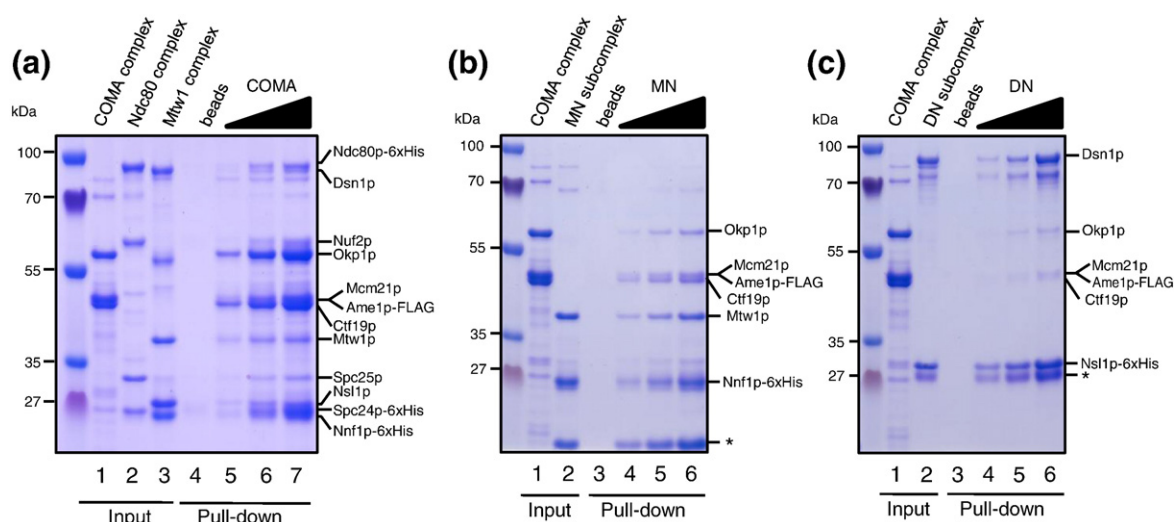
Fig. 6. Ndc80 and the COMA complex bind noncompetitively to the Mtw1 complex. (a) The COMA–FLAG complex (lane 1) was immobilized on M2 beads. Mtw1 complexes (lane 2) and Ndc80 complexes (lane 3) were premixed and incubated with control beads (lane 4) or COMA–FLAG. After the bound complexes had been washed, they were eluted with FLAG peptide (lanes 5–7). (b) Pull-down experiment using the 6×His-tagged MN subcomplex on Ni-NTA agarose and the FLAG-tagged COMA complex. Note the coelution of the complexes from the Ni-NTA beads. Asterisk indicates the Nnf1 truncation product. (c) Pull-down experiment using the 6×His-tagged DN subcomplex on Ni-NTA agarose and the FLAG-tagged COMA complex. The COMA complex fails to interact with the DN subcomplex. Asterisk denotes the Nsl1 truncation product.

critical binding motif (PVIHL) and a C-terminal tail, which is necessary for the interaction between human Nsl1 and the Ndc80 complex.[29] Instead, the binding interface between Mtw1 complexes and Ndc80 complexes seems to receive significant contributions from Mtw1 and/or Nnf1. These findings highlight the necessity to analyze kinetochores biochemically in evolutionarily distinct organisms in order to reveal common architectural principles and local binding interfaces.

Our results extend the studies of Maskell *et al.* and Petrovic *et al.* to provide a potential inner centromere receptor for the Mtw1 complex. The precise molecular basis for the interaction with the yeast Ctf19/COMA complex remains to be investigated. A puzzling aspect is that there is a considerably lower copy number of Ctf19 complex subunits (one to two) *versus* Mtw1 complexes (six to seven) for each budding yeast kinetochore, as judged by fluorescence microscopy.[5] Furthermore, only OKP1 and AME1 are essential genes in budding yeast.[30] It will be important to dissect in detail the molecular binding interface between Ctf19/COMA complexes and Mtw1 complexes and to evaluate the disruption of this binding interface *in vivo*. There may be considerable flexibility in the way the KMN network is anchored to the inner centromere. Some organisms such as *C. elegans* or *Drosophila melanogaster* seem to lack proteins entirely related to the CCAN.[2] In these kinetochores, the Mtw1 complex may rely on direct interactions with CENP-C for recruitment to the inner centromere.

Materials and Methods

Cloning of polycistronic expression vectors for Mtw1 and CTF19

Open reading frames corresponding to Mtw1 complex subunits were amplified from yeast genomic DNA, cloned, and expressed using the polycistronic expression system pET3aTr/pST39, which had been described previously.[31] Genes were subcloned from the monocistronic pET3aTr vector into the polycistronic cassettes (1–4) of pST39 in the following order for the Mtw1 complex: (1) MTW1, (2) NSL1, (3) NNF1-6×His, and (4) DSN1. The truncated version DSN$^{172–576}$ was cloned into pET28a(+) and expressed in combination with pST39 (MTW1-NSL1-NNF1-6×His).

The Ctf19/COMA subcomplex was cloned in the following order into the pST39 plasmid: (1) CTF19, (2) MCM21, (3) OKP1, and (4) AME1-6×His/FLAG. Because of the presence of an intron, MCM21 was amplified from yeast cDNA.

Protein expression and purification

The Mtw1 complex was expressed in BL21(DE3) (Novagen) for 4 h at 37 °C after induction at an OD$_{600}$ of 0.6 with 0.4 mM isopropyl-β-D-thiogalactopyranoside (IPTG). Coexpression with DSN$^{172–576}$ was performed overnight in the presence of 0.2 mM IPTG. The Mtw1 subcomplexes MN and DN were cloned into cassettes 1 and 2 of the pST39 vector, and the expression conditions were 37 °C for 4 h (MN) and 18 °C overnight (DN). The COMA subcomplex was expressed at 18 °C overnight after induction with 0.2 mM IPTG.

Bacteria were lysed by sonication in the presence of protease inhibitors (Roche), and the fusion proteins were isolated using Ni-NTA agarose beads (Qiagen). Binding and subsequent washing were performed in 20 mM Hepes (pH 7.0), 300 mM NaCl, and 30 mM imidazole. The Mtw1 complex or its two subcomplexes were eluted from Ni-NTA beads with 20 mM Tris (pH 8.5), 80 mM NaCl, and 250 mM imidazole; subsequently, they were subjected to anion-exchange chromatography using a MonoQ 5/50 GL column (GE Healthcare) The column was developed with 10 bed volumes of a linear gradient from 80 mM to 1 M NaCl in 20 mM Tris (pH 8.5) containing 5% glycerol. The DN subcomplex was further purified using SEC on a Superose 6 10/30 column.

The COMA–6×His subcomplex was purified with Ni-NTA agarose beads or Anti-FLAG M2 Affinity Gel (Sigma Aldrich). COMA–6×His was eluted with 20 mM Hepes (pH 7), 150 mM NaCl, 5% glycerol, and 250 mM imidazole, and loaded onto a SEC Superdex 200 HiLoad 16/60 column equilibrated in 20 mM Hepes (pH 7), 150 mM NaCl, and 5% glycerol. COMA–FLAG was eluted from M2 Affinity Gel with 3× FLAG peptide in Tris-buffered saline (TBS), and the complex was concentrated using ultrafiltration (10,000 molecular weight cutoff; Vivaspins), followed by buffer exchange into 20 mM Hepes (pH 7.0), 150 mM NaCl, and 5% glycerol using PD-10 columns (GE Healthcare). Protein concentration was determined with DC Protein Assay kit (Bio-Rad Laboratories).

The Ndc80 and Dam1 kinetochore complexes were expressed and purified as described previously.[9,11,24]

Interaction studies

The kinetochore protein complex (0.1–1 μM) in 500 μl of binding buffer was immobilized on 20 μl of Anti-FLAG M2 Affinity Gel or 20 μl of Ni-NTA agarose beads. The interaction partner to be tested was used at 1 μM in binding buffer (TBS or phosphate-buffered saline containing 30 mM imidazole). After incubation for 1 h at 4 °C, the beads were washed three times in either TBS with 0.1% (vol/vol) NP-40 or phosphate-buffered saline with 30 mM imidazole, and the complexes were specifically eluted with 3× FLAG peptide or 250 mM imidazole.

Electron microscopy

The Mtw1 complex was thawed and prepared for EM analysis by the GraFix method.[32] One hundred fifty micrograms of the complex was layered onto a 5–40% glycerol gradient in 20 mM Hepes (pH 7.6), 100 mM NaCl, 1 mM ethylenediaminetetraacetic acid, and 1 mM DTT (which also contained a 0.02–0.15% glutaraldehyde gradient), and ultracentrifuged at 55,000 rpm for 13 h in a TLS55 rotor at 4 °C. Fractions were analyzed by SDS-PAGE, and the fraction containing the monomeric cross-linked complex was applied to a glow-discharged C-flat grid (Protochips) augmented with a layer of thin carbon and stained with 2% uranyl formate.

Images were collected on a Gatan 4000 × 4000 charge-coupled device camera using a Tecnai F20 electron microscope operating at 120 kV and at a magnification of 30,000×. Despite purification by glycerol gradient, the images contained a mixture of aggregates and fragments, as well as the monodispersed full complex. Approximately 5000 particles that appeared to correspond to the full monomeric complex were picked manually with the BOXER program[33] and subjected to reference-free classification, as described previously.[34]

Coiled-coil predictions were performed with the MAR-COIL program.[35] The regions indicated with gray boxes in Fig. 2c correspond to areas of greater than 50% coiled-coil probability, all of which contain regions of greater than 80% coiled-coil probability.

Supplementary Data

Supplementary data associated with this article can be found, in the online version, at doi:10.1016/j.jmb.2010.11.012

References

1. Cheeseman, I. M. & Desai, A. (2008). Molecular architecture of the kinetochore–microtubule interface. *Nat. Rev. Mol. Cell Biol.* **9**, 33–46.
2. Santaguida, S. & Musacchio, A. (2009). The life and miracles of kinetochores. *EMBO J.* **28**, 2511–2531.
3. Tanaka, T. U., Rachidi, N., Janke, C., Pereira, G., Galova, M., Schiebel, E. *et al.* (2002). Evidence that the Ipl1–Sli15 (Aurora kinase–INCENP) complex promotes chromosome bi-orientation by altering kinetochore–spindle pole connections. *Cell*, **108**, 317–329.
4. Musacchio, A. & Salmon, E. D. (2007). The spindle-assembly checkpoint in space and time. *Nat. Rev. Mol. Cell Biol.* **8**, 379–393.
5. Joglekar, A. P., Bouck, D. C., Molk, J. N., Bloom, K. S. & Salmon, E. D. (2006). Molecular architecture of a kinetochore–microtubule attachment site. *Nat. Cell Biol.* **8**, 581–585.
6. Westermann, S., Drubin, D. G. & Barnes, G. (2007). Structures and functions of yeast kinetochore complexes. *Annu. Rev. Biochem.* **76**, 563–591.
7. Westermann, S., Wang, H. W., Avila-Sakar, A., Drubin, D. G., Nogales, E. & Barnes, G. (2006). The Dam1 kinetochore ring complex moves processively

on depolymerizing microtubule ends. *Nature*, **440**, 565–569.

8. Ciferri, C., Pasqualato, S., Screpanti, E., Varetti, G., Santaguida, S., Dos Reis, G. *et al.* (2008). Implications for kinetochore–microtubule attachment from the structure of an engineered Ndc80 complex. *Cell*, **133**, 427–439.

9. Westermann, S., Avila-Sakar, A., Wang, H. W., Niederstrasser, H., Wong, J., Drubin, D. G. *et al.* (2005). Formation of a dynamic kinetochore–microtubule interface through assembly of the Dam1 ring complex. *Mol. Cell*, **17**, 277–290.

10. Miranda, J. J., De Wulf, P., Sorger, P. K. & Harrison, S. C. (2005). The yeast DASH complex forms closed rings on microtubules. *Nat. Struct. Mol. Biol.* **12**, 138–143.

11. Lampert, F., Hornung, P. & Westermann, S. (2010). The Dam1 complex confers microtubule plus end-tracking activity to the Ndc80 kinetochore complex. *J. Cell Biol.* **189**, 641–649.

12. Tien, J. F., Umbreit, N. T., Gestaut, D. R., Franck, A. D., Cooper, J., Wordeman, L. *et al.* (2010). Cooperation of the Dam1 and Ndc80 kinetochore complexes enhances microtubule coupling and is regulated by aurora B. *J. Cell Biol.* **189**, 713–723.

13. Cheeseman, I. M., Chappie, J. S., Wilson-Kubalek, E. M. & Desai, A. (2006). The conserved KMN network constitutes the core microtubule-binding site of the kinetochore. *Cell*, **127**, 983–997.

14. Goshima, G., Kiyomitsu, T., Yoda, K. & Yanagida, M. (2003). Human centromere chromatin protein hMis12, essential for equal segregation, is independent of CENP-A loading pathway. *J. Cell Biol.* **160**, 25–39.

15. Cheeseman, I. M., Niessen, S., Anderson, S., Hyndman, F., Yates, J. R., III, Oegema, K. & Desai, A. (2004). A conserved protein network controls assembly of the outer kinetochore and its ability to sustain tension. *Genes Dev.* **18**, 2255–2268.

16. Kline, S. L., Cheeseman, I. M., Hori, T., Fukagawa, T. & Desai, A. (2006). The human Mis12 complex is required for kinetochore assembly and proper chromosome segregation. *J. Cell Biol.* **173**, 9–17.

17. De Wulf, P., McAinsh, A. D. & Sorger, P. K. (2003). Hierarchical assembly of the budding yeast kinetochore from multiple subcomplexes. *Genes Dev.* **17**, 2902–2921.

18. Kiyomitsu, T., Obuse, C. & Yanagida, M. (2007). Human Blinkin/AF15q14 is required for chromosome alignment and the mitotic checkpoint through direct interaction with Bub1 and BubR1. *Dev. Cell*, **13**, 663–676.

19. Wang, H. W., Long, S., Ciferri, C., Westermann, S., Drubin, D., Barnes, G. & Nogales, E. (2008). Architecture and flexibility of the yeast Ndc80 kinetochore complex. *J. Mol. Biol.* **383**, 894–903.

20. Joglekar, A. P., Bloom, K. & Salmon, E. D. (2009). *In vivo* protein architecture of the eukaryotic kinetochore with nanometer scale accuracy. *Curr. Biol.* **19**, 694–699.

21. Wei, R. R., Al-Bassam, J. & Harrison, S. C. (2007). The Ndc80/HEC1 complex is a contact point for kinetochore–microtubule attachment. *Nat. Struct. Mol. Biol.* **14**, 54–59.

22. Obuse, C., Iwasaki, O., Kiyomitsu, T., Goshima, G., Toyoda, Y. & Yanagida, M. (2004). A conserved Mis12 centromere complex is linked to heterochromatic HP1 and outer kinetochore protein Zwint-1. *Nat. Cell Biol.* **6**, 1135–1141.

23. Kiyomitsu, T., Iwasaki, O., Obuse, C. & Yanagida, M. (2010). Inner centromere formation requires hMis14, a trident kinetochore protein that specifically recruits HP1 to human chromosomes. *J. Cell Biol.* **188**, 791–807.

24. Westermann, S., Cheeseman, I. M., Anderson, S., Yates, J. R., III, Drubin, D. G. & Barnes, G. (2003). Architecture of the budding yeast kinetochore reveals a conserved molecular core. *J. Cell Biol.* **163**, 215–222.

25. Foltz, D. R., Jansen, L. E., Black, B. E., Bailey, A. O., Yates, J. R., III & Cleveland, D. W. (2006). The human CENP-A centromeric nucleosome-associated complex. *Nat. Cell Biol.* **8**, 458–469.

26. Okada, M., Cheeseman, I. M., Hori, T., Okawa, K., McLeod, I. X., Yates, J. R., III *et al.* (2006). The CENP-H-I complex is required for the efficient incorporation of newly synthesized CENP-A into centromeres. *Nat. Cell Biol.* **8**, 446–457.

27. Wan, X., O'Quinn, R. P., Pierce, H. L., Joglekar, A. P., Gall, W. E., DeLuca, J. G. *et al.* (2009). Protein architecture of the human kinetochore microtubule attachment site. *Cell*, **137**, 672–684.

28. Maskell, D. P., Hu, X. W. & Singleton, M. R. (2010). Molecular architecture and assembly of the yeast kinetochore MIND complex. *J. Cell Biol.* **190**, 823–834.

29. Petrovic, A., Pasqualato, S., Dube, P., Krenn, V., Santaguida, S., Cittaro, D. *et al.* (2010). The MIS12 complex is a protein interaction hub for outer kinetochore assembly. *J. Cell Biol.* **190**, 835–852.

30. Ortiz, J., Stemmann, O., Rank, S. & Lechner, J. (1999). A putative protein complex consisting of Ctf19, Mcm21, and Okp1 represents a missing link in the budding yeast kinetochore. *Genes Dev.* **13**, 1140–1155.

31. Tan, S. (2001). A modular polycistronic expression system for overexpressing protein complexes in *Escherichia coli*. *Protein Expression Purif.* **21**, 224–234.

32. Kastner, B., Fischer, N., Golas, M. M., Sander, B., Dube, P., Boehringer, D. *et al.* (2008). GraFix: sample preparation for single-particle electron cryomicroscopy. *Nat. Methods*, **5**, 53–55.

33. Ludtke, S. J., Baldwin, P. R. & Chiu, W. (1999). EMAN: semiautomated software for high-resolution single-particle reconstructions. *J. Struct. Biol.* **128**, 82–97.

34. Ramey, V. H., Wang, H. W. & Nogales, E. (2009). Ab initio reconstruction of helical samples with heterogeneity, disorder and coexisting symmetries. *J. Struct. Biol.* **167**, 97–105.

35. Delorenzi, M. & Speed, T. (2002). An HMM model for coiled-coil domains and a comparison with PSSM-based predictions. *Bioinformatics*, **18**, 617–625.